

An Electrochemical Path toward Pentaporphyrins

Laurent Ruhlmann, Sylvie Lobstein, Maurice Gross, and Alain Giraudeau*

Laboratoire d'Electrochimie et de Chimie Physique du Corps Solide, U.M.R. No. 7512, CNRS, Université Louis Pasteur, 4 rue Blaise Pascal, F-67000 Strasbourg, France

Received October 21, 1998

The porphyrins have long attracted chemists' interests because of their biological importance. Thus, considerable effort has been devoted to designing new materials that incorporate porphyrins as molecular building blocks. Synthetic porphyrin-based model systems are particularly relevant to the probing of effects of molecular organization on electronic communication; therefore, various chemical synthetic strategies have been proposed to create large arrays of covalently linked porphyrins subunits.¹

Redox chemistry can play an important role in the generation of new materials and in redox-controlled self-assembly, but to our knowledge only one report² presents an electrochemical synthesis of meso-meso-linked arrays. Recent results have demonstrated the general utility of electrochemical coupling as a powerful and versatile approach to the preparation of new porphyrinic assemblies.³ We report here an efficient two-step electrochemical coupling strategy that enables the preparation of pentameric blocks of porphyrins. The particular arrangement of the reported homomeric pentamer induces a clear difference in the redox characteristics of the central and peripheral porphyrin subunits.

In this preparative approach, the controlled electrochemical oxidation of zinc octaethylporphyrin, ZnOEP, in the presence of 4,4'-bipyridine (4,4'-bipy) as nucleophile, leads to the formation of the corresponding tetra-meso-substituted porphyrin bearing four 4,4'-bipyridiniums as substituents. The resulting porphyrin is the precursor in the synthesis of the target pentaporphyrin, which is obtained in an independent second step where this precursor reacts as a nucleophile with electrochemically generated ZnOEP⁺ π -cation radicals. The exhaustive electrochemical oxidations were performed under standard conditions previously reported.³ In the first oxidation step, a solution of ZnOEP (1 equiv) was oxidized

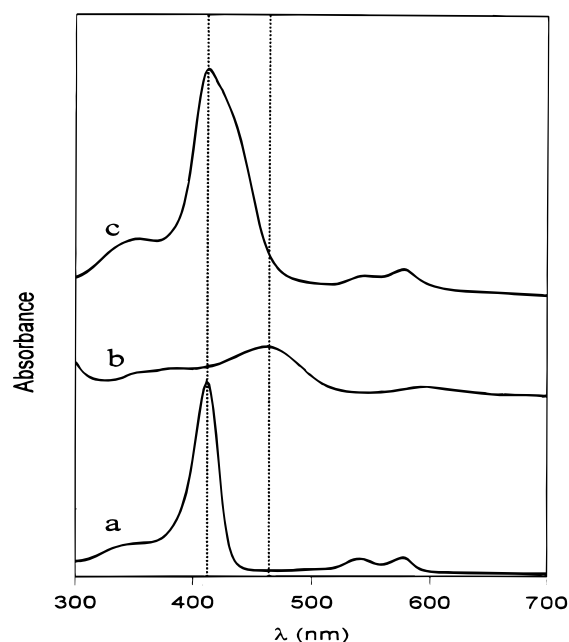


Figure 1. UV-vis absorption spectra: (a) ZnOEP-*meso*-bipy⁺ (see ref 3b), (b) $\alpha,\beta,\gamma,\delta$ -Zn, and (c) pentamer $\alpha,\beta,\gamma,\delta$ -Zn₅. Relative concentrations: (a) 1.0, (b) 1.0, and (c) 0.5.

in the presence of the nucleophile 4,4'-bipy (20 equiv). After the working potential was maintained at +1.20 V vs SCE for 2 days, the product of the electrolysis was isolated and characterized as the tetra-meso-substituted zinc porphyrin ($\alpha,\beta,\gamma,\delta$ -ZnOEP-(bipy⁺)₄) in 85% yield, ($\alpha,\beta,\gamma,\delta$ -Zn in Scheme 1).

In the second step, electrolysis of ZnOEP at +0.70 V vs SCE in the presence of $\alpha,\beta,\gamma,\delta$ -ZnOEP(bipy⁺)₄ gave the pentamer (Scheme 1), namely $\alpha,\beta,\gamma,\delta$ -ZnOEP-*meso*-(V²⁺-*meso*-ZnOEP)₄ ($\alpha,\beta,\gamma,\delta$ -Zn₅ in Scheme 1 with 76% yield).

UV-vis absorption spectra (Figure 1) showed that the precursor $\alpha,\beta,\gamma,\delta$ -Zn exhibited a significant red shift of the Soret (B) and visible (Q) bands compared to the corresponding unsubstituted porphyrin.^{3b} This bathochromic shift resulted from the electron-withdrawing effect of the four *meso*-bipyridinium cations on the porphyrin.⁴ In addition, the Soret band showed a dramatic decrease of its intensity and an important broadening. The Soret band of the pentamer $\alpha,\beta,\gamma,\delta$ -Zn₅ showed a large band splitting, and its absorption coefficient was approximately one half of the expected value (Figure 1), suggesting substantial excitonic coupling between the chromophores.⁵

The ¹H NMR spectra were consistent with the structures assigned. For the precursor $\alpha,\beta,\gamma,\delta$ -ZnOEP(bipy⁺)₄, ¹H NMR confirmed the absence of protons at the meso positions. The bipyridinium protons appeared downfield, respectively, as two doublets and two doubled doublets. The ethyl proton signals appeared as one quartet and

* To whom correspondence should be addressed.

(1) (a) Mongin, O.; Papamicaël, C.; Hoyler, N.; Gossauer, A.; *J. Org. Chem.* **1998**, *63*, 5568–5580. (b) Jaquinod, L.; Siri, O.; Khany, G. R.; Smith, K. M. *J. Chem. Soc., Chem. Commun.* **1998**, 1261–1262. (c) Khoury, R. G.; Jaquinod, L.; Aoyags, K.; Almstead, M. M.; Fisher, A. J.; Smith, K. M. *Angew. Chem.* **1997**, *109*, 2604–2606. (d) Osuka, A.; Shimidzu, H. *Angew. Chem., Int. Ed. Engl.* **1997**, *36*, 135–138. (e) Seth, J.; Palaniappan, V.; Johnson, T. E.; Prathapan, S.; Lindsey, J. S.; Bocian, D. F. *J. Am. Chem. Soc.* **1994**, *116*, 10578–10592. (f) Prathapan, S.; Johnson, T. E.; Lindsey, J. S. *J. Am. Chem. Soc.* **1993**, *115*, 7519–7520. (g) Wennerström, O.; Ericsson, H.; Raston, I.; Svensson, S.; Pimlott, W. *Tetrahedron Lett.* **1989**, *30*, 1129–1132. (h) Davila, J.; Harriman, A.; Milgrom, L. R. *Chem. Phys. Lett.* **1987**, *130*, 427–430. (i) Milgrom, L. R. *J. Chem. Soc., Perkin Trans. 1* **1983**, 2535–2539.

(2) Ogawa, T.; Nishimoto, Y.; Yoshida, N.; Ono, N.; Osuka, A. *J. Chem. Soc., Chem. Commun.* **1998**, 337–338.

(3) (a) Ruhlmann, L.; Giraudeau, A. *J. Chem. Soc., Chem. Commun.* **1996**, 2007–2008. (b) Giraudeau, A.; Ruhlmann, L.; El Kahef, L.; Gross, M. *J. Am. Chem. Soc.* **1996**, *118*, 2969–2979.

(4) (a) Hirota, J.; Okura, I. *J. Phys. Chem.* **1993**, *97*, 6867–6870. (b) Giraudeau, A.; Callot, H. J.; Jordan, J.; Ezahr, I.; Gross, M. *J. Am. Chem. Soc.* **1979**, *101*, 3857–3862.

(5) (a) Kasha, M.; Rawls, H. R.; El Bayoumi, M. A. *Pure Appl. Chem.* **1965**, *11*, 371–392. (b) McRae, E. G.; Kasha, M. *J. Chem. Phys.* **1958**, *28*, 721–722. (c) Felton, R. H.; Gouterman, M. *J. Chem. Phys.* **1964**, *41*, 2280–2286. (d) Shipman, L. L.; Norris, J. R.; Katz, J. J. *J. Phys. Chem.* **1976**, *80*, 877–882.

Scheme 1

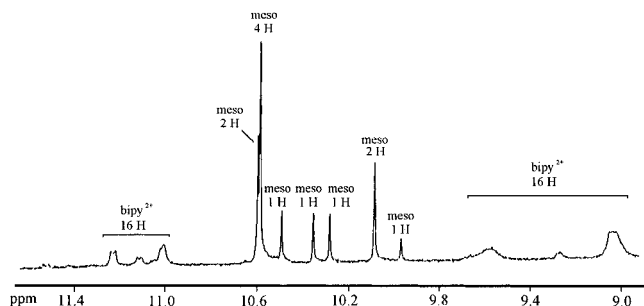
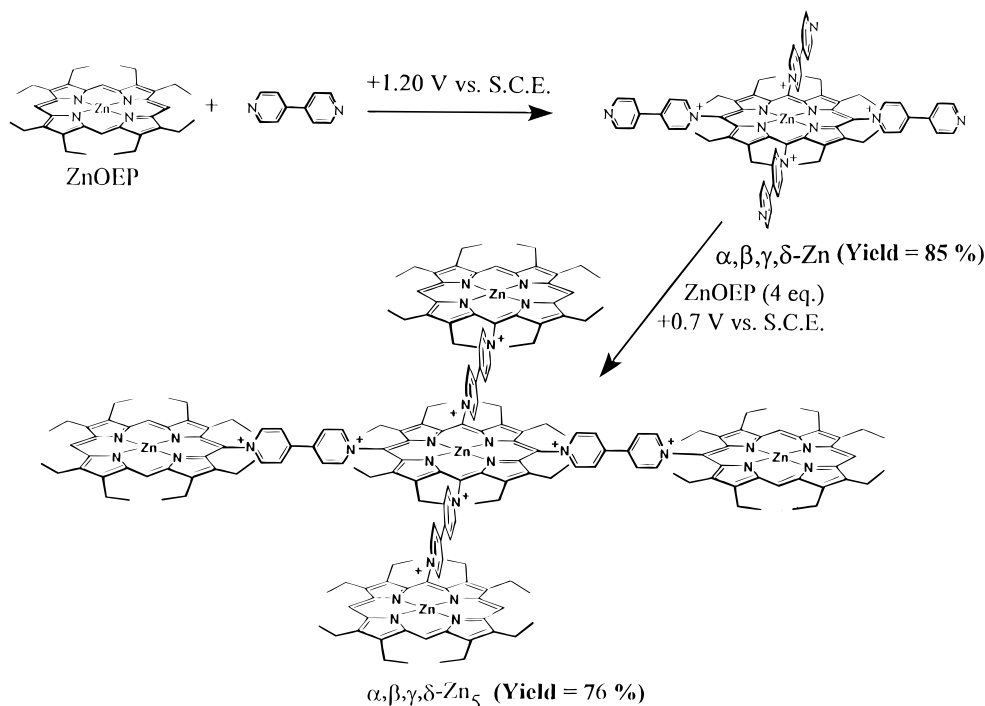


Figure 2. ^1H NMR of the pentaporphyrin $\alpha,\beta,\gamma,\delta\text{-Zn}_5$ (300 MHz, Py-d_5), aromatic region of the spectrum.

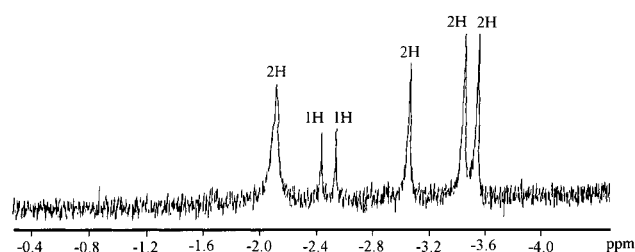


Figure 3. NH proton signals in the ^1H NMR spectrum of $\alpha,\beta,\gamma,\delta\text{-H}_{10}$ (300 MHz, $(\text{CD}_3)_2\text{CO}$).

one triplet in the range of 2.10–0.60 ppm, indicating that all the ethyls are equivalent and therefore that the porphyrin is symmetrical.

The pentamers $\alpha,\beta,\gamma,\delta\text{-M}$ ($\text{M} = \text{H}_{10}$ or Zn_5) gave very well-resolved ^1H NMR spectra (Figure 2). The observed ^1H NMR signals could be analyzed in two sets: the first one corresponded to porphyrinic protons (*meso*-H and ethyl) and the second one to the viologen protons. Surprisingly, the four peripheral porphyrin subunits of the pentamer were not equivalent. Only two of these four porphyrins resonated identically. The two others were shifted, respectively, downfield and high field. For each external porphyrin, two different types of *meso*-H signals

were also observed, in accord with the proposed meso-monosubstitution. These two singlets, which integrated in the ratio 2:1, appeared to be diagnostic of transannular monosubstitution on a meso position. Similar results were observed with the viologen proton signals.

For the demetalated pentamer $\alpha,\beta,\gamma,\delta\text{-H}_{10}$, the inner NH proton signals appeared as six different singlets (Figure 3) and confirmed the nonequivalence of the four peripheral porphyrin subunits. These results could suggest some degree of interactions between the porphyrin subunits.

Redox studies of the tetrasubstituted precursor have shown that, in addition to the typical oxidations and reductions of the porphyrin,^{6,7} four distinct one-electron transfers occurred that corresponded to the successive reductions of the four 4,4'-bipy⁺ substituents (Table 1). These observed splitting for the reduction of the 4,4'-bipy⁺ substituents indicated they were interacting. The anodic shifts observed both in the reduction and the oxidation steps of the porphyrin were consistent with the electron-withdrawing properties⁸ of the substituents, more pronounced in their oxidized than in their reduced state.

For the pentamer, the four viologens showed only two distinct reduction steps at -0.04 V (4e) and -0.57 V (4e) vs SCE, respectively, which were characteristic of their simultaneous reduction.⁹ The four peripheral porphyrins were oxidized and reduced in two steps, each involving

(6) (a) Fuhrhop, J. H.; Mauzerall, D. *J. Am. Chem. Soc.* **1969**, *91*, 4174–4181. (b) Wolberg, A.; Manassen, J. *J. Am. Chem. Soc.* **1970**, *92*, 2982–2991. (c) Antipas, A.; Dolphin, D.; Gouterman, M.; Johnson, E. C. *J. Am. Chem. Soc.* **1978**, *100*, 7705–7709.

(7) (a) Fuhrhop, J.H.; Kadish, K. M.; Davis, D. G. *J. Am. Chem. Soc.* **1973**, *95*, 5140–5147. (b) Stanienda, A. *Z. Phys. Chem.* **1964**, *229*, 259–266. (c) Fajer, J.; Borg, D. C.; Forman, A.; Dolphin, D.; Felton, R. H. *J. Am. Chem. Soc.* **1970**, *92*, 3451–3459. (d) Dolphin, D.; Muljiani, Z.; Rousseau, K.; Borg, D.C.; Fajer, J.; Felton, R. H. *Ann. N.Y. Acad. Sci.* **1973**, *206*, 117–119.

(8) (a) Kadish, K. M.; Morrison, M. M. *Inorg. Chem.* **1976**, *15*, 980–987. (b) Giraudeau, A.; Louati, A.; Gross, M.; Callot, H. J.; Hanson, L. K.; Rhodes, R. K.; Kadish, K. M. *Inorg. Chem.* **1982**, *21*, 1581–1586.

Table 1. Electrochemical Data for the Porphyrins Studied^a

porphyrins	ring oxidation			reduction of 4,4'-bipy ⁺ or bipy ²⁺	ring reduction				
	$E_{1/2}^{\text{III}}$	$E_{1/2}^{\text{II}}$	$E_{1/2}^{\text{I}}$		$E_{1/2}^{\text{I}}$	$E_{1/2}^{\text{II}}$	$E_{1/2}^{\text{III}}$	$E_{1/2}^{\text{IV}}$	
ZnOEP		0.94	0.68		-1.60				
$\alpha,\beta,\gamma,\delta$ - Zn		1.47 ^{irr}	1.27 ^{irr}	-0.34 ^b	-1.26 ^b	-1.41 ^b			
				-0.48 ^b					
				-0.71 ^b					
				-0.82 ^b					
$\alpha,\beta,\gamma,\delta$ - Zn₅	1.35 ^{irr}	<u>1.19^{irr}</u> (5e)	0.97(4e)	-0.04(4e) ^b	-0.57(4e) ^b	-0.83 ^b	-1.10 ^b	-1.61(4e) ^b	-1.80(4e) ^b

^a Voltammetry in CH₃CN/1,2-C₂H₄Cl₂ (1:4), Et₄NPF₆ 0.1 M. Working electrode: Pt. All potentials in V vs SCE. All steps were reversible one-electron transfers except those with brackets identifying the number of electrons transferred. The underlined potential corresponded both to the first oxidation step of the four peripheral porphyrin (4 × 1e) and the second oxidation step of the internal porphyrin (1 × e).

^b Potential obtained by polarography (dropping mercury electrode).

four electrons (1e per molecule). As expected, the oxidation potentials of the central subunit shifted about 0.2V more positive than those of the peripheral subunits.³

A more striking electrochemical property of the pentamer was the dramatic decrease in the HOMO–LUMO gap (taken as $\Delta E = E_{1/2}^{\text{ox}} - E_{1/2}^{\text{red}}$ of the first oxidation and reduction) relative to the central porphyrin (which was $\Delta E = 2.02$ V in the pentamer vs $\Delta E = 2.53$ V in the precursor). This block design with viologen-bridged porphyrins thus represented a chromophore system with highly stabilized 1e reduced and oxidized forms. Unprecedented, the central porphyrin became easily reducible (first reduction at -0.83 V) compared to the similar peripheral porphyrins (first reduction at -1.61 V). This feature indicated a strong electron-accepting character of this central subunit in the pentamer. Interestingly, these characteristics demonstrated the feasibility of building a pentameric porphyrins block where two electrons may be specifically addressed to the central porphyrin subunit.

In summary, an efficient electrosynthetic path has been devised for the synthesis of a fully substituted zinc octaethylporphyrin as a precursor, allowing the synthesis of a pentaporphyrin in an independent second step. This method has the key advantage of allowing the synthesis of a porphyrin block involving a central subunit whose electronic properties markedly differ from those of the four peripheral chromophores. In addition, these differences can be easily modulated by changing the cation in the central subunit and/or by substitution on the periphery of the porphyrins. Therefore, this electrochemical synthetic strategy, based on a building block approach, in which zinc octaethylporphyrins were linked via viologen groups on the meso positions, provides an easy entry to a new class of multiporphyrin arrays. Such molecular architectures thus offer the likely possibility of developing light-harvesting devices.

Experimental Section

I. Materials. All solvents and chemicals were of reagent grade quality, purchased commercially, and used without further purification except as noted below. CH₂Cl₂ for use in exhaustive electrolysis was heated at reflux with and distilled from CaH₂. The supporting electrolyte tetraethylammonium hexafluorophosphate (Et₄NPF₆) was used without further purification. ZnOEP was purchased from Aldrich Chemical Co. Thin-layer chromatography (TLC) was performed on commercially prepared alumina or silica gel plates purchased from Roth Sochiel.

(9) (a) Elafsen, R. M.; Edsberg, R. L. *Can. J. Chem.* **1957**, *35*, 646–650. (b) Osa, T.; Kuwana, T. *J. Electroanal. Chem.* **1969**, *22*, 389–406. (c) Bard, A. J. *Adv. Phys. Org. Chem.* **1976**, *13*, 155–278. (d) Wüm, G. S.; Berneth, H. *Top. Curr. Chem.* **1980**, *92*, 1–44.

II. Apparatus. All electrochemical measurements have been carried out under argon. Voltammetric data were obtained with a standard three-electrodes system using a Bruker E 130 M potentiostat and a high-impedance millivoltmeter (minisis 6000, Tacussel). Current-potential curves were obtained from an Itelec If 3802 X-Y recorder. The working electrode was a platinum disk (E.D.I. type, Solea Tacussel) of 3.14 mm² surface area. A platinum wire was used as the auxiliary electrode. The reference electrode was a saturated calomel electrode (SCE) that was electrically connected to the studied solution by a junction bridge filled with the corresponding solvent-supporting electrolyte solution. For polarographic and differential pulse polarographic experiments, a signal generator (GSATP from Solea-Tacussel) was associated with a potentiostatic device (Solea-Tacussel) comprising a potentiostat (PRT 20-2X) and a voltage pilot unit (Servovit).

Coulometric measurements and quantitative electrochemical synthesis were performed in a standard 100 mL cell. The working electrode was a platinum wire ($\varnothing = 0.8$ mm) of 60 cm length. For the controlled-potential electrolysis, the anodic and cathodic compartments were separated by a fritted glass disk to prevent diffusion of the electrogenerated species.

UV-visible spectra were recorded on a Shimadzu UV-260 spectrophotometer.

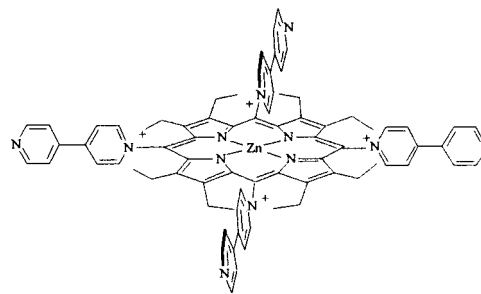
¹H NMR spectra were obtained in (CD₃)₂CO, CD₃CN, or Py-d₅ on a Bruker A.C. 300 (300 Mhz) spectrometer.

Elementary analyses were performed by the microanalysis services of Institut Charles Sadron or Chemical Department of I.U.T. Strasbourg Sud.

III. Synthesis. Electrochemical Synthesis. General Procedure. Prior to electrolysis, the corresponding mixtures were stirred and degassed by bubbling argon through the solution for 10 min. Then, the desired working potential was applied. During anodic oxidation, the electrolyzed solution was continuously stirred and maintained under argon. After electrolysis, solvents were removed by rotary evaporator. The residue was dissolved in a minimum of CH₂Cl₂, and then the mixture was poured into water and the organic layer was washed twice.

Typical preparation and characterization of a substituted monomer and of a pentaporphyrin are reported hereafter.

$\alpha,\beta,\gamma,\delta$ -**Zn**. ZnOEP (50 mg, 0.084 mmol) and 524 mg of 4,4'-bipyridine (3.35 mmol) were dissolved in 100 mL of CH₂Cl₂/CH₃CN (4/1) 0.1 M Et₄NPF₆ solution. The electrolysis was carried

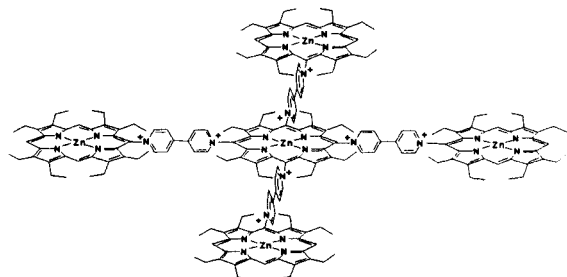


out during 72 h at + 1.20 V vs SCE. After treatment, the organic extract was concentrated (~10 mL) and chromatographed on alumina. The first fraction (eluted with CH₂Cl₂/C₂H₅OH, 96/4) was a mixture of bisubstituted and trisubstituted porphyrin. The desired product was eluted with a mixture of CH₂Cl₂/C₂H₅OH

(92/8). After evaporation of the solvent, $\alpha,\beta,\gamma,\delta$ -Zn was recrystallized from CH_2Cl_2 and *n*-hexane to give violet-blue crystals (128 mg, 0.071 mmol), yield 85%. $\alpha,\beta,\gamma,\delta$ -Zn was dried under vacuum at 120 °C during 48 h: UV-vis ($\text{CH}_2\text{Cl}_2/\text{DMF}$, 99/1) λ_{max} , nm (ϵ , $\text{M}^{-1}\cdot\text{cm}^{-1}$) 462 (55 800), 590 (12 500); $^1\text{H NMR}$ (300 MHz, $\text{CD}_3\text{-CN}$, 25 °C) δ 11.32 (d, $J_0 = 6.4$ Hz, 8 H, 4,4'-bipy $^+$), 9.42 (d, $J_0 = 6.4$ Hz, 8 H, 4,4'-bipy $^+$), 9.16 (d, $J_0 = 6.4$ Hz, 8 H, 4,4'-bipy $^+$), 8.26 (d, $J_0 = 6.4$ Hz, 8 H, 4,4'-bipy $^+$), 2.05 (q, $^3J = 7.2$ Hz, 16 H, 8 CH_2 of $-\text{CH}_2\text{CH}_3$), 0.65 (t, $^3J = 7.2$ Hz, 24 H, 8 CH_3 of $\text{CH}_2\text{-CH}_3$); MS (FAB $^+$, NBA) m/z 1798.7 ($\text{C}_{76}\text{H}_{72}\text{N}_{12}\text{Zn}(\text{PF}_6)_4^+$), 1653.7 ($\text{C}_{76}\text{H}_{72}\text{N}_{12}\text{Zn}(\text{PF}_6)_3^+$), 1507.7 ($[\text{C}_{76}\text{H}_{72}\text{N}_{12}\text{Zn}(\text{PF}_6)_2 - \text{H}]^+$), 1362.7 ($[\text{C}_{76}\text{H}_{72}\text{N}_{12}\text{Zn}(\text{PF}_6) - \text{H}]^+$); mp >300 °C.

Anal. Calcd for $\text{C}_{76}\text{H}_{72}\text{N}_{12}\text{Zn}(\text{PF}_6)_4$ ($M = 1798.73$ g·mol $^{-1}$): C, 50.74; H, 4.03; N, 9.35. Found: C, 50.84; H, 4.39; N, 9.12.

Pentaporphyrin $\alpha,\beta,\gamma,\delta$ -Zn $_5$. ZnOEP (41 mg, 0.068 mmol) and 30 mg of $\alpha,\beta,\gamma,\delta$ -Zn (0.017 mmol) were dissolved in 100 mL of 1,2- $\text{C}_2\text{H}_4\text{Cl}_2/\text{CH}_3\text{CN}$ (4/1), 0.1 M Et_4NPF_6 mixture. The



electrolysis was carried out at +0.70 V vs SCE during 72 h. After treatment, the organic extract was chromatographed on a silica gel column (Kieselgel, 230–400 mesh). The first fraction (elution with CH_2Cl_2) gave unoxidized ZnOEP. Further elution with $\text{CH}_2\text{Cl}_2/\text{CH}_3\text{OH}$ (94/6) gave the pentamer $\alpha,\beta,\gamma,\delta$ -Zn $_5$. After evaporation of the solvent, $\alpha,\beta,\gamma,\delta$ -Zn $_5$ was recrystallized from CH_2Cl_2 , *n*-hexane to give black red crystals (62 mg, 0.013 mmol): yield 76%; UV-vis ($\text{CH}_2\text{Cl}_2/\text{CH}_3\text{OH}$, 99/1) λ_{max} , nm (ϵ , $\text{M}^{-1}\cdot\text{cm}^{-1}$) 412 (446 000), 544 (39 300), 578 (52 000); $^1\text{H NMR}$ (300 MHz, Py-d_5 , 25 °C) δ 11.25–10.95 (m, 16 H, H of bipy $^{2+}$), 10.59 (s, 2 H, meso H), 10.58 (s, 4 H, meso H), 10.48 (s, 1 H, meso H), 10.34

(s, 1 H, meso H), 10.27 (s, 1 H, meso H), 10.07 (s, 2 H, meso H), 9.95 (s, 1 H, meso H), 9.70–9.49 (m, 8 H, H of bipy $^{2+}$), 9.28–9.22 (m, 2 H, H of bipy $^{2+}$), 9.10–8.93 (m, 6 H, H of bipy $^{2+}$), 4.31–3.90 (m, 52 H, 26 CH_2 , Et), 3.80 (q, $^3J = 7.2$ Hz, 12 H, 6 CH_2 , Et), 2.50–2.30 (m, 12 H, 6 CH_2 , Et), 2.23 (q, $^3J = 7.0$ Hz, 6 H, 2 CH_3 , Et), 2.01–1.80 (m, 78 H, 26 CH_3 , Et), 1.66 (t, $^3J = 7.2$ Hz, 18 H, 6 CH_3 , Et), 1.41 (m, 18 H, 6 CH_3 , Et), 0.79 (t, $^3J = 7.00$ Hz, 6 H, 2 CH_3 , Et). Anal. Calcd for $\text{C}_{220}\text{H}_{244}\text{N}_{28}\text{Zn}_5(\text{PF}_6)_8$ ($M = 4766.90$ g·mol $^{-1}$): C, 55.43; H, 5.16; N, 8.23; Zn, 6.86. Found: C, 55.78; H, 5.22; N, 8.12; Zn, 7.02.

Pentaporphyrin $\alpha,\beta,\gamma,\delta$ -H $_{10}$. Hydrochloric acid (25%, 100 mL) was added to an acetone solution of $\alpha,\beta,\gamma,\delta$ -Zn $_5$, and the mixture was stirred for 30 min at room temperature. After addition of 200 mL of water, the organic layer was separated, washed with water, and neutralized with saturated sodium acetate solution. The solution was washed with water again, dried over CaSO_4 , and evaporated. Recrystallization of the residue gave $\alpha,\beta,\gamma,\delta$ -H $_{10}$ in almost quantitative yield: UV-vis ($\text{CH}_2\text{Cl}_2/\text{CH}_3\text{OH}$, 99/1) λ_{max} , nm (ϵ , $\text{M}^{-1}\cdot\text{cm}^{-1}$) 405 (240 200), 506 (40 800), 538 (29 700), 571 (22 900), 623 (18 200); $^1\text{H NMR}$ (300 MHz, $(\text{CD}_3)_2\text{CO}$, 25 °C) δ 10.60–10.53 (m, 16 H, H of bipy $^{2+}$), 10.59 (s, 4 H, meso H), 10.57 (s, 1 H, meso H), 10.52 (s, 2 H, meso H), 10.18 (s, 1 H, meso H), 10.17 (s, 1 H, meso H), 9.86 (s, 2 H, meso H), 9.73–9.56 (m, 9 H, H of bipy $^{2+}$ + 1 meso H), 9.08–8.98 (m, 8 H, H of bipy $^{2+}$), 4.29–3.93 (m, 52 H, 26 CH_2 , Et), 3.75 (q, $^3J = 7.35$ Hz, 12 H, 6 CH_2 , Et), 2.58 (q, $^3J = 7.35$ Hz, 12 H, 6 CH_2 , Et), 2.19 (q, $^3J = 7.71$ Hz, 4 H, 2 CH_2 , Et), 2.01–1.65 (m, 72 H, 24 CH_3 , Et), 1.62 (t, $^3J = 7.35$ Hz, 6 H, 2 CH_3 , Et), 1.42 (t, $^3J = 7.35$ Hz, 18 H, 6 CH_3 , Et), 0.93 (t, $^3J = 7.35$ Hz, 18 H, 6 CH_3 , Et), 0.68 (t, $^3J = 7.71$ Hz, 6 H, 2 CH_3 , Et), –2.07 (s, 2 H, NH peripheral OEP), –2.41 (s, 1 H, NH OEP central), –2.51 (s, 1 H, NH OEP central), –3.02 (s, 2 H, NH peripheral OEP), –3.41 (s, 2 H, NH peripheral OEP), –3.56 (s, 2 H, NH peripheral OEP); mp >300 °C. Anal. Calcd for $\text{C}_{220}\text{H}_{254}\text{N}_{28}(\text{PF}_6)_8$ ($M = 4450.12$ g·mol $^{-1}$): C, 59.37; H, 5.75; N, 8.81. Found: C, 59.71; H, 6.13; N, 8.43.

Acknowledgment. We warmly thank the Centre National de la Recherche Scientifique for financial support.

JO982119K